BIOCHEMICAL PHARMACOLOGY 77 (2009) 228–237

available at www.sciencedirect.com

ScienceDirect

journal homepage: www.elsevier.com/locate/biochempharm

In vivo profiling of DPP4 inhibitors reveals alterations in collagen metabolism and accumulation of an amyloid peptide in rat plasma

Marco M. Jost [a], *Jens Lamerz* [a], *Harald Tammen* [a,*], *Christoph Menzel* [b], *Ingrid De Meester* [c], *Anne-Marie Lambeir* [c], *Koen Augustyns* [c], *Simon Scharpé* [c], *Hans Dieter Zucht* [d], *Horst Rose* [e], *Michael Jürgens* [a], *Peter Schulz-Knappe* [d], *Petra Budde* [d]

[a] *Digilab BioVisioN GmbH, Feodor-Lynen-Street 5, 30625 Hannover, Germany*
[b] *QIAGEN GmbH, QIAGEN Street 1, 40724 Hilden, Germany*
[c] *University of Antwerp, Campus Drie Eiken, Department of Pharmaceutical Sciences, Universiteitsplein 1, B-2610 Antwerp, Belgium*
[d] *Proteome Sciences R&D GmbH & Co KG, Altenhöferallee 3, 60438 Frankfurt, Germany*
[e] *ImVisioN GmbH, Feodor-Lynen-Street 5, 30625 Hannover, Germany*

ARTICLE INFO

Article history:
Received 26 August 2008
Accepted 22 September 2008

Keywords:
BRI peptide
Peptidomics
Differential peptide display
Dipeptidyl peptidase 4
Type 2 diabetes
Vildagliptin

ABSTRACT

Dipeptidyl peptidase 4 (DPP4) inhibitors represent a novel class of oral anti-hyperglycemic agents. The complete pharmacological profile of these protease inhibitors remains unclear. In order to gain deeper insight into the in vivo effects caused by DPP4 inhibition, two different DPP4 inhibitors (vildagliptin and AB192) were analyzed using differential peptide display. Wistar rats were treated with the DPP4 inhibitors (0.3 mg kg^{-1}; 1 mg kg^{-1} or 3 mg kg^{-1} body weight) and DPP4 activity was measured before and at the end of the experiment. One hour after compound administration, blood plasma samples were collected to generate peptide displays and to subsequently identify differentially regulated peptides. A dose-dependent decrease in blood plasma DPP4 activity was measured for both inhibitors. DPP4 inhibition influenced collagen metabolism leading to depletion of collagen derived peptides (e.g. collagen alpha 1 (III) 521–554) and accumulation of related N-terminally extended collagen derived peptides (e.g. collagen alpha 1 (III) 519–554). Furthermore, the intact amyloid rat BRI (1–23) peptide was detected in plasma following in vivo DPP4 inhibition. DPP4 catalyzed cleavage kinetics of the BRI peptide were determined in vitro. The k_{cat} and K_m for cleavage by DPP4 were 5.2 s^{-1} and 14 μM, respectively, resulting in a specificity constant k_{cat}/K_m of 0.36×10^6 s^{-1} M^{-1}. Our results demonstrate that differential peptide analysis can be applied to monitor action of DPP4 inhibition in blood plasma. For the first time effects on basal collagen metabolism following DPP4 inhibition in vivo were demonstrated and the BRI amyloid peptide was identified as a novel DPP4 substrate.

* *Corresponding author*. Tel.: +49 511 538896 57; fax: +49 511 536696 66.
E-mail address: h.tammen@peptidomics.com (H. Tammen).

Abbreviations: BRI, integral membrane protein 2B processed active peptide 244-266; DPD, differential peptide display; DPP4, dipeptidyl peptidase 4; ESI, electrospray ionization; k_{cat}, enzymatic catalytic rate; MALDI, matrix-assisted laser desorption/ionization; MMP, matrix-metalloprotease; MS/MS, tandem mass spectrometry; *m/z*, mass-to-charge ratio; SI, signal intensity; qTOF, quadrupole time of flight; TFA, trifluoroacetic acid; TGF β1, transforming growth factor β1.

0006-2952/$ – see front matter © 2008 Elsevier Inc. All rights reserved.
doi:10.1016/j.bcp.2008.09.032

1. Introduction

Dipeptidyl peptidase 4 (DPP4) inhibitors such as sitagliptin and vildagliptin represent a new class of antidiabetic agents that improve glycemic control by preventing glucagon-like peptide-1 (GLP-1) and glucose-dependent insulinotropic polypeptide (GIP) degradation. These intestinal peptides, also known as incretins, are postprandially secreted from enteroendocrine L- and K-cells and lead to a rise in insulin secretion. Preclinical [1–4] and clinical studies [5–11] show that inhibition of DPP4 decreases blood glucose levels but long-term data on efficiency and safety are lacking. Several other peptides were identified in vitro as efficient DPP4 substrates, including chemokines (e.g. stromal cell derived factor 1 alpha or CXCL12, MDC or CCL22, and RANTES or CCL5), pancreatic polypeptide family members (e.g. neuropeptide Y), as well as diverse other substrates (e.g. endomorphin, kentsin). The in vivo relevance of these findings is not clear at the moment, but needs to be investigated [12–15]. Blocking N-terminal truncation of peptides by DPP4 inhibition might lead to accumulation of the corresponding substrate and hence influence, for example, downstream mediated receptor signaling events. To evaluate the potential pharmacological effects of in vivo DPP4 inhibition independently of its glucose lowering properties and to identify physiological substrates of DPP4, we subcutaneously treated Wistar rats with two different DPP4 inhibitors – the experimental, irreversible inhibitor AB192, and the clinically used, reversible inhibitor vildagliptin – and evaluated endogenous blood plasma peptides using differential peptide display, which allows the identification of multiple changes in blood plasma composition on the peptide level (<15 kDa) using a combination of reverse phase HPLC, offline MALDI-MS and a bioinformatic data analysis. Signals of interest are sequenced and identified to elucidate DPP4 inhibitor related effects and evaluate pharmacological responses caused by therapeutic intervention. In contrast to in vitro experiments where inhibitors are tested usually against selected proteases or proteases against limited sets of possible substrates (peptide libraries), in vivo protease inhibitor profiling allows to test their action against all endogenous proteases and influences on natural substrates [16]. Similar to our approach, Yates et al. [17] used differential mass spectrometry for identifying substrates of DPP4 and aminopeptidase P2 in human plasma in vitro. Using this technique, we identified the BRI peptide as DPP4 substrate in rat plasma and were able to show for the first time the influence of DPP4 inhibition on the collagen metabolism in vivo.

2. Materials and methods

Reagents if not otherwise specified were purchased from Sigma–Aldrich, Munich, Germany.

2.1. DPP4 inhibitors and animals

Bis(4-acetamidophenyl) 1-(S)-prolylpyrrolidine-2(R,S)-phosphonate (AB192) was synthesized as described previously [18] and 1-[[(3-hydroxy-1-adamantyl)amino]acetyl]-2-cyano-(S)-pyrrolidine (vildagliptin) [4] was synthesized by GL Synthesis Inc. (Worchester, MA, USA). Animal experiments were performed by Phenos GmbH (Hannover, Germany) according to European Directive 86/609/EEC on animal experimentation. Male Wistar rats were purchased from Charles River (Sulzfeld, Germany) at 7 weeks of age, housed in a temperature-, humidity-, and light-controlled room (21–23 °C, 12–12 h light dark cycle) and given free access to food and water.

2.2. DPP4 inhibition in vivo

Eight-week-old Wistar rats (315–320 g) were treated with the DPP4 inhibitors (AB192/vildagliptin) or received vehicle (50 mmol l^{-1} sodium phosphate buffer; pH 7.4) into the fat tissue of the neck using a 27-G needle. The study setup for two independently performed experiments, was as follows. In a first set of experiments, a total of eight rats per treatment group received either vehicle, 0.3 mg kg^{-1}; 1 mg kg^{-1} or 3 mg kg^{-1} body weight AB192 or vildagliptin, respectively. In a second set of experiments, 4 rats received 3 mg kg^{-1}, 8 rats received 1 mg kg^{-1} and 12 rats received 0.3 mg kg^{-1} body weight. Vehicle was given to a total of 12 rats. Blood samples (100 μl) for DPP4 activity measurements were drawn from the tail vein before the application and at the end of the experiment (+60 min). At this point the rats were anesthetized by a mixture of ketamine 10% (Bremer Pharma, Warburg, Germany; 0.9 mg kg^{-1} body weight) and ROMPUN™ 2% (Bayer Vital, Leverkusen, Germany; 0.02 mg kg^{-1} body weight). Additionally, rats received a short burst of ether for quick narcosis. The thorax was opened immediately and 4–6 ml of blood were taken from the right ventricle into an EDTA laminated syringe and transferred into a 15 ml Falcon-tube filled with 2.5 mg ml^{-1} EDTA.

2.3. Measurement of DPP4 activity

Blood samples taken from the tail vein were immediately centrifuged (2000 × *g*; 10 min at RT) and plasma stored at −20 °C. At the day of the measurement, 10 μl of each sample were pipetted in duplicates directly in a 96-well plate (placed on ice). After all samples and standards (0–0.5 mU ml^{-1} purified DPP4-enzyme from porcine kidney) were pipetted, 40 μl of freshly prepared substrate solution (500 μmol l^{-1} Gly-Pro-4-nitroanilide diluted in 40 mmol l^{-1} HEPES-buffer, pH 7.4) were added to each well. Immediately, the absorbance (405 nm) was followed at 37 °C over a period of 1 h (microtiterplate reader Tecan GENios, Crailsheim, Germany). Blanks (plasma + HEPES-buffer) were subtracted from the measured sample values and the DPP4 activity in units $liter^{-1}$ [U l^{-1}] calculated using the standard calibration.

2.4. Preparation of plasma samples for differential peptide display

Blood taken from the right ventricle as described above was processed under strictly standardized conditions. Samples were centrifuged (RT) for 10 min at 2000 × *g*; the plasma was subsequently spun for 15 min at 2500 × *g*. Platelet poor plasma was stored immediately at −80 °C. Proteins were removed by centrifugal ultrafiltration and peptide displays generated as described previously [19]. Briefly, after protein

depletion a 750 μl equivalent of plasma was separated into 96 distinct fractions by reverse phase liquid chromatography. After separation each fraction was subjected to MALDI-TOF-mass spectrometry (Applied Biosystems 4700 Proteomics Analyzer, Framingham, MA, USA) in the linear mode. The mass spectra of all fractions generated from one sample were visualized in a 2D gel-like format, termed peptide display. Thus, each peak is depicted as a bar with its color intensity corresponding to the intensity of the corresponding MALDI-peak. The *x*-, *y*- and *z*-axis represent mass-to-charge ratios (*m*/*z*), chromatographic fraction and mass spectrometric signal intensity, respectively. Mass intervals range from 1000 to 15,000 *m*/*z* ratios.

2.5. Determination of peptide coordinates and peptide signal intensities

For each of the 96 individual fractions an averaged spectrum was computed from a total of 124 samples of the corresponding mass spectrum, resulting in a mean peptide display. This served as a template for the definition of coordinates (chromatographic fraction and *m*/*z*) of 10,560 mass spectrometric signals. After baseline correction of the spectra, signal intensities at these coordinates were determined in all samples and stored in a data matrix.

2.6. Statistical data analysis

For each signal coordinate the significance of the relation signal intensity to inhibitor dose (dose response) was determined by computing the Spearman's rank correlation coefficients *r* and considered to be significant if $|r|$ exceeded a threshold equivalent to a probability of error $\alpha \leq 5\%$ [20]. Signal candidates of interest required significant correlation in the AB192 dose response (AB192 targets), in the vildagliptin dose response (vildagliptin targets), or both (common targets).

2.7. Identification by nESI-qTOF MS/MS

Selected peptides were identified by nESI-qTOF MS/MS (QSTAR pulsar, Applied Biosystems/MDS Sciex, Toronto, Canada) with subsequent protein database searching. The resulting peptide fragment spectra were produced in the product ion scan mode (spray voltage 950 V, collision energy 28 eV). Up to 200 scans per selected precursor ion were accumulated. Data processing prior to database searching included charge state deconvolution (Bayesian reconstruct tool of the BioAnalyst program package; Sciex) and de-isotoping (customized Analyst QS macro; Sciex). The resulting spectra were saved in Mascot (Matrix Science, London, UK) generic file format and submitted to the Mascot search engine. Cascading searches including several posttranslational modifications in Swissprot (Version 41, www.expasy.ch) and MSDB (Version 030212, EBI, Europe) were performed by the Mascot Daemon client software (Version 1.9, Matrix Science).

2.8. Identification by MALDI-MS/MS

For MALDI-MS/MS experiments, the sample/matrix mixture was spotted on a hydrophobic stainless steel target (OptiTOF plates, Applied Biosystems, Framingham, MA, USA). Survey MALDI-TOF-MS spectra were acquired in a fully automated fashion in the reflector mode of a 4700 proteomics analyzer (Applied Biosystems). All measurements were calibrated using a daily updated default calibration. Precursor selection for MS/MS experiments was performed by "on-the-fly" spectra evaluation of the MS spectra typically using a signal-to-noise ratio higher than 30 and a precursor mass smaller than 4000 Da as inclusion criteria. Fragmentation of native peptides was carried out in the CID mode of the MALDI-TOF/TOF mass spectrometer with collision energy of 1 keV and ambient air as the collision gas at a typical pressure of 4×10^{-7} torr. MS/MS spectra were subsequently noise filtered and peak de-isotoped using the Data Explorer software (Applied Biosystems, V. 4.4) before submission to the Mascot database search engine as described above.

2.9. In vitro degradation of human BRI and its inhibition

Human BRI amyloid peptide (1–23) was obtained from Bachem (Weil am Rhein, Germany). For the experiments using plasma as protease source, the BRI peptide was dissolved in 90% TFA resulting in a stock solution of 320 $\mu mol\,l^{-1}$. Aliquots were further diluted with double distilled water (1 $\mu mol\,l^{-1}$) and 3.6 or 7.2 μl of this solution incubated with 1.2 ml of human blood plasma with or without AB192 inhibitor (50 $\mu mol\,l^{-1}$) at 37 °C for 30 min. The reaction was terminated by adding 8 $mol\,l^{-1}$ guanidine hydrochloride up to a total volume of 4.8 ml. Samples were stored at −80 °C and ultracentrifugation performed as described above and peptide displays generated.

The kinetic analysis was carried out using DPP4 purified from human seminal plasma as reported elsewhere [21]. The specific activity of the enzyme was 35 U mg^{-1}. One unit (U) of DPP4 activity is the amount of enzyme required to catalyze the conversion of one micromole of substrate per minute in presence of 0.5 $mmol\,l^{-1}$ Gly-Pro-4-nitroanilide and 50 $mmol\,l^{-1}$ Tris buffer, pH 8.3 at 37 °C.

The truncation kinetics of BRI were measured essentially as described by Lambeir et al. [22]. Shortly, DPP4 was mixed with substrate and incubated at 37 °C in presence of 50 $mmol\,l^{-1}$ Tris/HCl buffer, pH 7.5, 1 $mmol\,l^{-1}$ EDTA. The final DPP4 activity was 25 $U\,l^{-1}$. The concentration dependency of the truncation rate was determined between 5 and 200 μM of peptide (eight concentrations, starting stock solution 1 mM BRI in water, freshly prepared).

At certain time intervals, samples were withdrawn and quenched with TFA. C18 ZipTips (Millipore Corp., Bedford, MA) were used to desalt the samples. Elution was performed step-wise with 30 and 50% acetonitrile in 0.1% acetic acid. The mixture of this combined elution was analyzed in an Esquire ESI Ion Trap mass spectrometer (Bruker, Bremen, Germany). The instrument was used in a normal range, normal resolution setting, optimized on an *m*/*z* value near the most abundant ion of the intact peptide. The concentrations of the intact and truncated peptides were calculated from their relative intensity. The initial rate of conversion was estimated from 3 time points (2, 4 and 8 or 4, 8 and 16 min). The results were directly fitted to the Michaelis–Menten equation.

3. Results

3.1. DPP4 inhibition in vivo

One hour after the administration of DPP4 inhibitors (AB192 and vildagliptin), Wistar rats showed a dose-dependent decrease in blood plasma DPP4 activity reaching a maximal inhibition of approximately 80% at 3 mg kg^{-1} body weight as displayed in Fig. 1. The data reveal that vildagliptin inhibits DPP4 activity already by ~50% at a dosage of 0.3 mg kg^{-1} body weight, whereas AB192 sufficiently inhibits DPP4 only in the higher dosage range (>1 mg kg^{-1} body weight). Similar results for vildagliptin were shown in studies using obese Zucker fa/fa rats [2,4].

3.2. Differential peptide display

To profile peptides in each individual sample by generating peptide displays, platelet free EDTA plasma was used. Using plasma in such a study is an important prerequisite since serum or residual platelets exhibit enzymatic activities, which are leading to an ex vivo generation of peptides, which hampers the sensitive detection of endogenously generated peptides [23]. From the 124 generated peptide displays, 7 samples were identified as technical outliers on the basis of visual inspection of the peptide displays and principal component analysis of the data matrix. They were excluded from further analysis. A mean peptide display (average of all mass spectra of each individual sample) contains a total of ~10,000 mass spectrometric signals, which correspond to approximately 3500 individual peptides. This reflects redundancy by peptides that elute in more than one fraction, multiple-charge states, peptide species with and without oxidative states, and a small number of mass spectrometric derivatives, such as fragment ions.

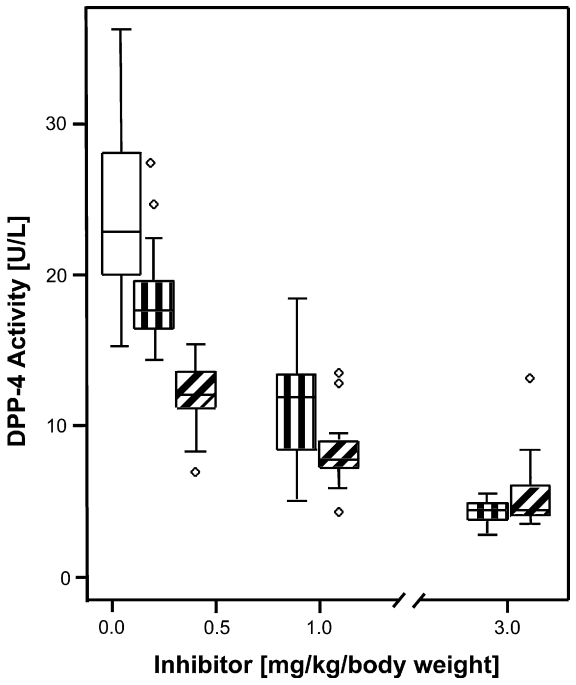

Fig. 1 – DPP4 activity of rat plasma samples. Following injection of the two inhibitors, a dose-dependent decrease in DPP4 activity was measured as described in Section 2. All of the tested doses led to a significant decrease in activity – with vildagliptin more potent already in the lower range. Significance was tested using the Man–Whitney *U*-test ($p < 0.05$). Hollow: vehicle; Diagonal: vildagliptin; Vertical: AB192; *y*-axis: DPP4 activity (U l^{-1}); *x*-axis: inhibitor dose (mg kg^{-1}).

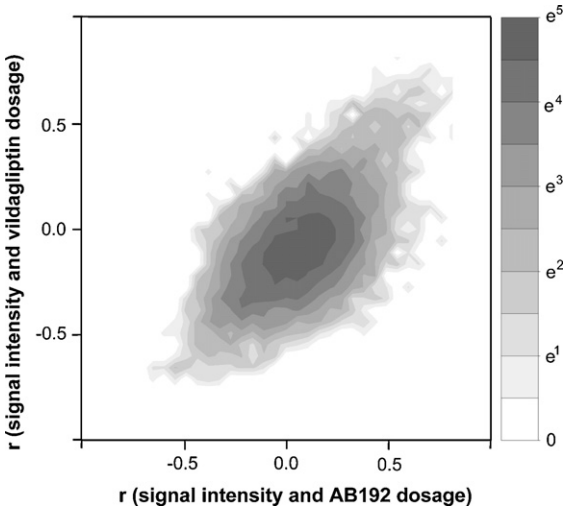

Fig. 2 – Contour plot representing the influence of the inhibitors AB192 and vildagliptin. The distribution of signals is plotted in dependence of their correlation values to the corresponding inhibitor (legend on the right). There is a clear diagonal trend from the lower left to the upper right of the contour plot, so that in general signals which are influenced by one inhibitor are more or less influenced by the other inhibitor, too. The majority of signals is not affected at all by the inhibitors (dark oval) corresponding to high density of signals around *r* (signal intensity and AB192 dosage) = 0 and *r* (signal intensity and vildagliptin dosage) = 0.

3.3. Influence of DPP4 inhibition on peptide signals

Under the given thresholds (as described in Section 2), 9% of the detected signals were significantly regulated by the applied DPP4 inhibitors AB192 and/or vildagliptin. After AB192 and vildagliptin treatment, 5.4 and 3.5% of the signals increased, while 0.1 and 2.1% decreased, respectively. The contour plot in Fig. 2 gives an impression of how the two inhibitors affect the peptide signals: The correlation of any peptide signal to the inhibitor dosage is represented towards the inhibitors AB192 (*x*-axis) and vildagliptin (*y*-axis). There is a clear diagonal trend from the lower left to the upper right of the contour plot, so that in general signals which are influenced by one inhibitor are more or less influenced by the other inhibitor, too.

3.4. Identification of regulated peptides

To reveal the nature of inhibitor induced changes, 19 signal coordinates of regulated peptides were sequenced and identified

Table 1 – Identified DPP4 substrates and products in rat plasma.

Index	*m/z*	Correlation coefficient		*p*-value		Protein precursor, amino acid range	Sequence, SwissProt. accession number (www.expasy.com)
		AB 192	vildagliptin	AB 192	vildagliptin		
1	2234	−0.303	−0.609	0.209	0.002	Collagen alpha 1 (I) chain (216–238)	**GPP_GKNGDDGEAGKPGRPGERGPPGP**_QGA (P02454)
2	2814	−0.233	−0.494	0.259	0.021	Collagen alpha 1 (I) chain (295–325)	**PRG_LPGERGRPGPPGSAGARGNDGAVGAAGPPGP**_TGP (P02454)
3	2805	0.554	0.598	0.003	0.000	Collagen alpha 1 (I) chain (802–832)	**PAG_FAGPPGADGQPGAKGEPGDTGVKGDAGPPGP**_AGP (P02454)
4	3493	−0.251	−0.672	0.026	0.000	Collagen alpha 1 (I) chain (804–843)	**GFA_GPPGADGQPGAKGEPGDTGVKGDAGPPGPAGPAGPPGPIG**_NVG (P02454)
5	2192	−0.328	−0.516	0.097	0.006	Collagen alpha 1 (I) chain (809–832)	**PGA_DGQPGAKGEPGDTGVKGDAGPPGP**_AGP (P02454)
6	3267	−0.305	−0.703	0.259	0.004	Collagen alpha 1 (I) chain (996–1030)	**GLA_GPPGESGREGSPGAEGSPGRDGAPGAKGDRGETGP**_AGP (P02454)
7	3210	−0.150	−0.603	0.383	0.009	Collagen alpha 1 (I) chain (997–1030)	**LAG_PPGESGREGSPGAEGSPGRDGAPGAKGDRGETGP**_AGP (P02454)
8	3333	0.582	0.621	0.002	0.001	Collagen alpha 1 (III) chain (519–554)	**PRG_VAGEPGRDGTPGGPGIRGMPGSPGGPGNDGKPGPPG**_SQG (P13941)
9	3132	−0.468	−0.629	0.026	0.000	Collagen alpha 1 (III) chain (521–554)	**GVA_GEPGRDGTPGGPGIRGMPGSPGGPGNDGKPGPPG**_SQG (P13941)
10	1938	−0.182	−0.409	0.209	0.009	Collagen alpha 1 (III) chain (665–686)	**GEA_GAPGVPGGKGDSGAPGERGPPG**_TAG (P13941)
11	2579	−0.371	−0.685	0.073	0.001	Collagen alpha 1 (III) chain (812–839)	**GFP_GAPGQNGEPGAKGERGAPGEKGEGGPPG**_AAG (P13941)
12	4922	−0.216	−0.585	0.620	0.001	Collagen alpha 1 (III) chain (1001–1053)	**GLP_GQPGTAGEPGRDGNPGSDGQPGRDGSPGGKGDRGENGSP-GAPGAPGHPGPPGP**_VGP (P13941)
13	4228	−0.375	−0.692	0.017	0.001	Collagen alpha 2 (I) chain (194–238)	**LDG_LKGQPGAQGVKGEPGAPGENGTPGQAGARGLPGERGRVGAPGPAG_ARG** (P02466)
14	2638	−0.284	−0.538	0.259	0.008	Collagen alpha 2 (I) chain (460–488)	**GLP_GSPGNVGPAGKEGPVGLPGIDGRPGPIGP**_AGP (P02466)
15	4086	−0.078	−0.598	0.383	0.004	Collagen alpha 2 (I) chain (649–692)	**GLP_GERGAAGIPGGKGEKGETGLRGEIGNPGRDGARGAPGAIGAPGP**_AGA (P02466)
16	2855	−0.335	−0.432	0.017	0.002	Collagen alpha 2 (I) chain (931–958)	**GEA_GRDGNPGSDGPPGRDGQPGHKGERGYPG**_NIG (P02466)
17	5490	0.734	0.062	0.002	0.612	Vitronectin (Somatomedin B) (20–67)	**ALA_DQESCKGRCTEGFNVDKKCQCDELCSYYQSCCTDYTAECKPQVTRGDV**_FTM (P04004.1)
18	2675	0.665	0.573	0.001	0.000	Integral membrane protein 2B (244–266)	**QKR_EASNCFTIRHFENKFAVETLICS** (Q5XIE8)
19	2475	−0.421	−0.575	0.029	0.014	Integral membrane protein 2B (246–266)	**REA_SNCFTIRHFENKFAVETLICS** (Q5XIE8)

The table shows the mass-to-charge ratios (*m/z*), the experimental group (AB192 or vildagliptin) with the corresponding correlation coefficient (signal intensity and inhibitor dosage) and *p*-value obtained by the Mann–Whitney *U*-test comparing groups of control and highest applied inhibitor dosage for each differentially regulated peptide. This is followed by the precursor name and sequence range, the amino acid sequence and the SwissProt accession number in parenthesis. The sequenced peptide is depicted in bold. Preceding and succeeding amino acids are depicted before and after the horizontal lines.

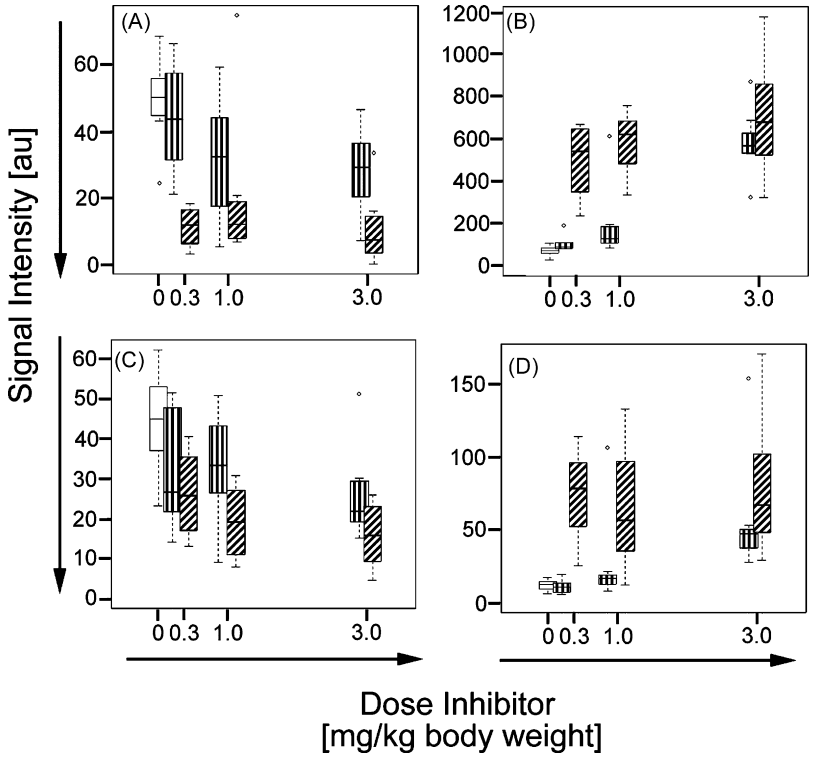

Fig. 3 – (A–D) Box-and-Whisker Plot of the dose response of regulated peptides following DPP4 inhibition. Signal intensities measured under vehicle treatment (hollow), and under increasing doses of AB192 (vertical) and vildagliptin (diagonal). Collagen alpha 1 (III) 521–554 (A) shows dose-dependent-depletion with increasing concentrations of both inhibitors, while collagen alpha 1 (III) 519–554 (B) shows dose-dependent accumulation. The truncated BRI (246–266) peptide (C) and intact BRI (244–266) peptide (D) are a further example of a substrate-product pair, where the DPP4 mediated amino-terminal proteolysis is dose-dependently inhibited by both inhibitors.

by means of ESI and MALDI-MS/MS (Table 1). A pronounced effect of DPP4 inhibition was observed on the level of collagen trimming and metabolism. For example, collagen peptides derived from the alpha 1 or alpha 2 collagen chain were significantly depleted following DPP4 inhibition with vildagliptin or AB192 (e.g. Table 1 #9 (Fig. 3A) and Table 1 #13). Thereby, the effect of vildagliptin was more pronounced – from the 14 depleted collagen peptide signals identified, all were significantly affected, whereas only 4 collagen peptides were significantly affected in plasma samples derived from rats treated with the AB192 inhibitor. Significant accumulation of a collagen peptide was shown for the collagen alpha 1 (I) chain peptide (802–832) (Table 1 #3) and collagen alpha 3 (I) chain peptide (519–554) (Table 1 #8 and Fig. 3B) which were detectable in plasma from vildagliptin as well as AB192 treated rats.

Furthermore, we identified a non-collagenous DPP4 substrate which is derived from the integral membrane protein 2B (ITM2B) also known as BRI [24]. The BRI peptide possesses the N-terminal DPP4 cleavage motif (EAS; Table 1 #18). We could trace the truncated BRI (3–23) 200 Da shorter form generated by DPP4 action in the control animals as wells as the intact BRI (1–23) form under AB192 and vildagliptin treatment (Fig. 3C and D, and Fig. 4). Additionally, we identified a vitronectin (20–67) peptide (Table 1 #17) in samples treated with AB192 but not with vildagliptin. This peptide contains the somatomedin B sequence (20–63) as well as cell attachment site (RGD 64–66). However, the N-terminal sequence (DQE) is not a DPP4 cleavage site.

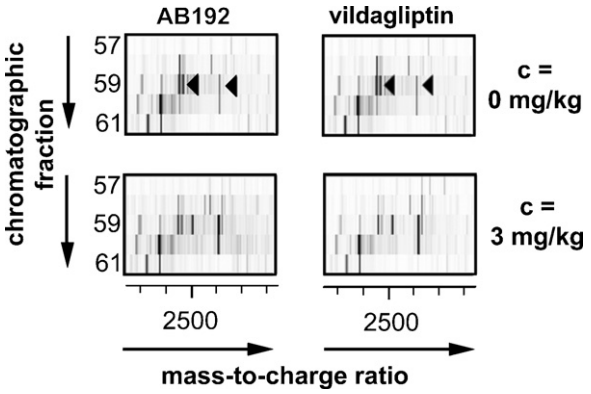

Fig. 4 – Effect of DPP4 inhibition on the BRI peptide. Peptide displays of samples treated with and without inhibitor (3 mg kg^{-1} body weight) were averaged. The mass spectrometric signal intensity in Fraction 59 with a mass-to-charge ratio (*m/z*) of 2475 (left arrow) decreases following inhibition, while the intensity in fraction 59 with *m/z* 2675 (right arrow) increases. The signals were identified by ESI-MS as Integral membrane protein 2B with start at position 246–266 (signal # 19 in Table 1) and 244–266 (signal # 18 in Table 1), respectively. The latter shows typical DPP4 cleavage recognition site and has the dose response of an accumulating DPP4 substrate, while the first peptide has lost an N-terminal dipeptide and performs like an accumulating product.

3.5. *In vitro degradation of BRI*

The human BRI (1–23) peptide, spiked into human plasma, is cleaved by the action of DPP4 and degradation is reduced by addition of AB192 (Fig. 5). In human plasma samples without exogenous human BRI (1–23) added and without AB192 inhibitor treatment, we could also detect the endogenously truncated BRI (3–23) peptide but not the intact BRI (1–23) peptide. The kinetic analysis using purified DPP4 and BRI peptide revealed a k_{cat} and K_m of 5.2 s^{-1} and 14 μM, respectively, resulting in a specificity constant k_{cat}/K_m of 0.36 × 10^6 s^{-1} M^{-1}.

4. Discussion

In the present study, we show that in vivo inhibition of DPP4 activity in rats using either the experimental irreversible DPP4 inhibitor AB192 or the clinically used inhibitor vildagliptin leads to pronounced effects on the collagen metabolism and accumulation of the so far unknown DPP4 substrate BRI in blood plasma. Thereby, vildagliptin appears to be the more potent inhibitor compared to AB192 by sufficiently inhibiting DPP4 activity already in the lower dosage range.

To the best of our knowledge, this is the first report showing that in vivo collagen degradation is affected by DPP4 inhibition. Since the discovery of DPP4 [25], a role of this protease in collagen metabolism was suggested as collagen contains numerous glycine–proline sequence stretches which are potential cleavage sites for DPP4 [26,27]. Furthermore, in vitro data suggest that DPP4 possesses substrate specificity for denatured collagen types I, II, III, and V [27], where, within collagen I, the alpha 1 (I) chain was found to be the most prominent binding ligand of DPP4 [28]. These findings are confirmed by our in vivo data showing that collagen peptides

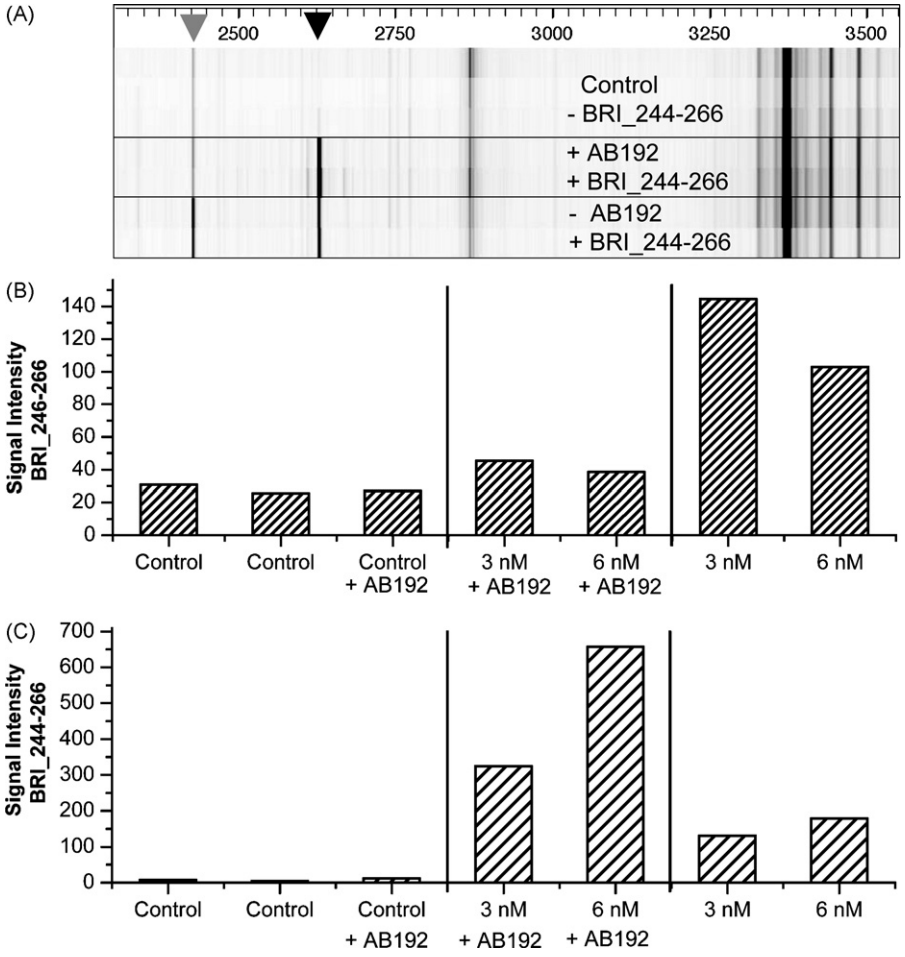

Fig. 5 – (A–C) Spiking and detection of BRI peptide and its truncated form in human plasma samples. Plasma samples were spiked with 3 nmol l^{-1} or 6 nmol l^{-1} human BRI peptide with or without AB192 and incubated for 30 min. Additionally, two passive controls (no spiking) and one active control (AB192 only) were generated. The lane view represents a distinct area from seven peptide displays with the same fraction and mass range (A). The grey arrow marks the signals of the truncated BRI (246–266) peptide and the black arrow marks its intact form (244–266). The graphs depict the corresponding signal intensities (B and C). The truncated form of the BRI peptide (246–266) is visible in the controls, as well as in the AB192 treated samples. The strongest signal is detectable in the samples spiked with the BRI (244–266) peptide without AB192 inhibitor added. Accumulation of BRI (244–266) peptide was detectable in the inhibitor AB192 treated samples and a depletion of BRI (244–266) peptide was measured if no inhibitor was added. In the controls BRI (244–266) peptide is not detectable.

derived from the triple helical region of the alpha 1 (I) collagen chains are depleted by the action of vildagliptin and AB192. This indicates that collagen trimming by DPP4 is prevented following inhibition leading to a depletion of the corresponding products. Similarly, peptides from the alpha 2 (I) and alpha 1 (III) collagen chain are also down regulated. Peptides identified from the collagen alpha chain are overlapped (collagen alpha 1 (I) chain (804–832) and collagen alpha 1 (I) chain (809–832), Table 1 #4 and #5). This might be explained by the observation that the collagen chains are cleaved by the action of matrix-metalloproteases (MMP) at different recognition sites [29–32]. This pre-digest of the collagen chains by MMP could be a prerequisite to allow DPP4 to act at the N-terminus of the generated collagen peptides. Additionally, we could detect that the collagen alpha 3 (I) chain (519–554) and the collagen alpha 1 (I) chain (802–832) peptides accumulate after DPP4-inhibitor treatment. The latter peptide shows the N-terminal sequence (GPP) indicating that this peptide is not further processed by DPP4 after cleavage of the N-terminal residues (FA).

For both DPP4 inhibitors, AB192 and vildagliptin, there was a significant correlation between the accumulating collagen derived peptides and the dosages. At the highest dose of vildagliptin used, the highest degree of inhibition was obtained. This was reflected by the most pronounced accumulation of collagen peptides containing the N-terminal DPPIV consensus motif. At this stage, we cannot exclude the possibility that the effects of AB192 and vildagliptin are, at least partially, mediated by other dipeptidyl peptidases or by other yet unknown targets. However, as the collagen peptides in vivo are most readily accessible to DPP4 (soluble or plasma membrane bound), it seems likely that interference with DPP4 is responsible for the observed changes.

At this time point, the long-term consequences of alterations of the collagen metabolism in vivo following DPP4 inhibition are unknown. However, DPP4 negative Fischer rats excrete elevated quantities of proline- and hydroxyproline-containing peptides in their urine indicating impaired collagen metabolism and experienced a significant weight loss when a proline-rich protein diet was fed [33,34]. Furthermore, blocking of DPP4 using DPP4 specific antibodies leads to proteinuria in Lewis rats [35]. Recent studies have additionally shown that blocking of DPP4-like activity with Lys[Z(NO2)]-thiazolidide and Lys[Z(NO2)]-pyrrolidide in vitro abrogates transforming growth factor β1 (TGF β1) induced collagen synthesis of human skin fibroblasts and keloid-derived skin fibroblasts and suppresses the profibrotic effect of TGF β1 in a mouse model of dermal fibrosis which is detected, among others, by collagen I expression [36]. Altogether, these data strongly support the view that type 2 diabetes patients treated with DPP4 inhibitors should be closely monitored regarding possible adverse events related to alterations in the collagen metabolism.

Since collagens represent the most abundant protein class in mammalians and contain a multitude of DPP4 consensus motifs, most of the regulated signals were identified as collagen derived. This finding complicates the identification of DPP4 substrates which are non-collagenous since the collagen derived peptides might mask other peptides which are biologically relevant yet non-abundant. Furthermore, several known DPP4 targets are only present in detectable amounts under a given stimulus (e.g. glucose challenge for GLP-1 or under inflammatory conditions like the chemokine RANTES) – the current threshold level for peptides detectable in plasma by the described method is 50 pmol l^{-1} [37,38]. Despite these difficulties, we were able to identify so far one non-collagenous DPP4 substrate which is derived from the integral membrane protein 2B also known as BRI [24]. It is thought that by the action of furin, a subtilisin-like proprotein convertase, a 23 amino acid long peptide is cleaved from the C-terminus of ITM2B (ITM2B 244–266; assigned as BRI amyloid peptide) [37]. In our experience, the kinetic parameters for BRI cleavage by DPP4 are in the same order of magnitude as for the endogenous substrate GLP-1 [38,39]. Moreover, the efficient Glu-Ala release is peculiar as most reported P_2-Ala substrates contain a basic or uncharged amino acid in the P_2 position. The Glu-Ala release from BRI is at least 100 times faster than the release of an Asp-Ala dipeptide from vasoactive intestinal peptide (3–28) by DPP4 [40]. The physiological role of the BRI peptide remains unclear but Kim et al. [41] demonstrated recently that the BRI amyloid peptide, present in human cerebrospinal fluid, inhibits amyloid β protein aggregation in vitro and mediates its anti-amyloidogenic effect in vivo. Furthermore, it is known that a mutated 34 amino acid long form of the BRI peptide which is known as ABri, is expressed not only in the brain of patients suffering from familial British dementia but is also present in serum in a soluble form. As a fibrillar component of amyloid deposits, it is also detectable in the blood vessels of several tissues, including pancreas and myocardium [42].

In rats treated with AB192 but not with vildagliptin, accumulation of a vitronectin (20–67) peptide was detected. As vitronectin (20–67) possesses a N-terminal sequence (DQE) which is not a DPP4 specific cleavage site, we concluded that vitronectin (20–67) is not a DPP4 substrate rather indicating a possible off-target effect caused by AB192. This differential influence illustrates that monitoring the effects of DPP4 inhibitors on plasma peptide composition may contribute to the identification of compound-specific effects in vivo.

In summary, we could show that peptides are suitable surrogates for altered protease activity and that differential peptide display is capable to detect alterations on the blood plasma peptidome caused by DPP4 inhibitors in vivo. Thus, the described methods circumvent the problem that results from in vitro data where cleavage of a given peptide by DPP4 is not necessarily transferable to the in vivo situation [43]. Future works should focus on the measurement of alterations in human plasma samples from type 2 diabetes patients treated with DPP4 inhibitors to gain deeper insights in drug action, to correlate accumulated substrates with secondary pharmacological effects and ultimately develop predictive markers for selection of suitable inhibitors for subpopulations of patients.

Acknowledgements

We gratefully acknowledge the superb technical assistance of Christina Grethe, Claudia Hubner, Michaela Brandt, Sigfried

Zimmermann, Kerstin Kupke, and Vincent Hanebuth (all Digilab BioVisioN GmbH, Hannover, Germany). This study was supported by a grant from the Bundesministerium für Bildung und Forschung (PTJ-BIO/Wir/0313624). Part of this work was presented on the 2nd International Conference on Dipeptidyl Aminopeptidases, Magdeburg, Germany (2005). ''Differential Peptide Display'', ''Peptidomics'', and ''Spectromania'' are trademarks of Digilab BioVisioN GmbH, Hannover, Germany.

REFERENCES

[1] Balkan B, Kwasnik L, Miserendino R, Holst JJ, Li X. Inhibition of dipeptidyl peptidase IV with NVP-DPP728 increases plasma GLP-1 (7–36 amide) concentrations and improves oral glucose tolerance in obese Zucker rats. Diabetologia 1999;42:1324–31.

[2] Burkey BF, Li X, Bolognese L, Balkan B, Mone M, Russell M, et al. Acute and chronic effects of the incretin enhancer vildagliptin in insulin-resistant rats. J Pharmacol Exp Ther 2005;315:688–95.

[3] Sudre B, Broqua P, White RB, Ashworth D, Evans DM, Haigh R, et al. Chronic inhibition of circulating dipeptidyl peptidase IV by FE 999011 delays the occurrence of diabetes in male zucker diabetic fatty rats. Diabetes 2002;51:1461–9.

[4] Villhauer EB, Brinkman JA, Naderi GB, Burkey BF, Dunning BE, Prasad K, et al. 1-[[(3-Hydroxy-1-adamantyl)amino]acetyl]-2-cyano-(S)-pyrrolidine: a potent, selective, and orally bioavailable dipeptidyl peptidase IV Inhibitor with antihyperglycemic properties. J Med Chem 2003;46:2774–89.

[5] Aschner P, Kipnes MS, Lunceford JK, Sanchez M, Mickel C, Williams-Herman DE. Effect of the dipeptidyl peptidase-4 inhibitor sitagliptin as monotherapy on glycemic control in patients with type 2 diabetes. Diabetes Care 2006;29:2632–7.

[6] Charbonnel B, Karasik A, Liu J, Wu M, Meininger G. Efficacy and safety of the dipeptidyl peptidase-4 inhibitor sitagliptin added to ongoing metformin therapy in patients with type 2 diabetes inadequately controlled with metformin alone. Diabetes Care 2006;29:2638–43.

[7] Nauck MA, Meininger G, Sheng D, Terranella L, Stein PP. Efficacy and safety of the dipeptidyl peptidase-4 inhibitor, sitagliptin, compared with the sulfonylurea, glipizide, in patients with type 2 diabetes inadequately controlled on metformin alone: a randomized, double-blind, non-inferiority trial. Diabetes Obes Metab 2007;9:194–205.

[8] Rosenstock J, Baron MA, Dejager S, Mills D, Schweizer A. Comparison of vildagliptin and rosiglitazone monotherapy in patients with type 2 diabetes: a 24-week, double-blind, randomized trial. Diabetes Care 2007;30:217–23.

[9] Schweizer A, Couturier A, Foley JE, Dejager S. Comparison between vildagliptin and metformin to sustain reductions in HbA(1c) over 1 year in drug-naive patients with Type 2 diabetes. Diabet Med 2007;24:955–61.

[10] Ahren B, Gomis R, Standl E, Mills D, Schweizer A. Twelve- and 52-week efficacy of the dipeptidyl peptidase IV inhibitor LAF237 in metformin-treated patients with type 2 diabetes. Diabetes Care 2004;27:2874–80.

[11] Dejager S, Razac S, Foley JE, Schweizer A. Vildagliptin in drug-naive patients with type 2 diabetes: a 24-week, double-blind, randomized, placebo-controlled, multiple-dose study. Horm Metab Res 2007;39:218–23.

[12] Green BD, Flatt PR, Bailey CJ. Dipeptidyl peptidase IV (DPP IV) inhibitors: a newly emerging drug class for the treatment of type 2 diabetes. Diab Vasc Dis Res 2006;3:159–65.

[13] Richter B, Bandeira-Echtler E, Bergerhoff K, Lerch C. Dipeptidyl peptidase-4 (DPP-4) inhibitors for type 2 diabetes mellitus. Cochrane Database Syst Rev 2008;CD006739.

[14] Brandt I, Lambeir AM, Maes MB, Scharpe S, De Meester I. Peptide substrates of dipeptidyl peptidases. Adv Exp Med Biol 2006;575:3–18.

[15] Lambeir AM, Durinx C, Scharpe S, De Meester I. Dipeptidyl-peptidase IV from bench to bedside: an update on structural properties, functions, and clinical aspects of the enzyme DPP IV. Crit Rev Clin Lab Sci 2003;40:209–94.

[16] Jost M, Budde P, Tammen H, Schulz-Knappe P. Peptidomics based protease inhibitor profiling. In: Gänshirt D, Harms F, Rohmann S, Schulz-Knappe P, editors. Peptidomics in drug development. Aulendorf, Germany: Editio Cantor; 2005. p. 65–73.

[17] Yates NA, Deyanova EG, Geissler W, Wiener MC, Sachs JR, Wong KK, et al. Identification of peptidase substrates in human plasma by FTMS based differential mass spectrometry. Int J Mass Spectrom 2007;259:174–83.

[18] Belyaev A, Zhang X, Augustyns K, Lambeir AM, De Meester I, Vedernikova I, et al. Structure-activity relationship of diaryl phosphonate esters as potent irreversible dipeptidyl peptidase IV inhibitors. J Med Chem 1999;42:1041–52.

[19] Tammen H, Schulte I, Hess R, Menzel C, Kellmann M, Mohring T, et al. Peptidomic analysis of human blood specimens: comparison between plasma specimens and serum by differential peptide display. Proteomics 2005;5:3414–22.

[20] Lamerz J, Selle H, Scapozza L, Crameri R, Schulz-Knappe P, Mohring T, et al. Correlation-associated peptide networks of human cerebrospinal fluid. Proteomics 2005;5:2789–98.

[21] de Meester I, Vanhoof G, Lambeir AM, Scharpe S. Use of immobilized adenosine deaminase (EC 3.5. 4. 4) for the rapid purification of native human CD26/dipeptidyl peptidase IV (EC 3. 4. 14. 5). J Immunol Methods 1996;189:99–105.

[22] Lambeir AM, Proost P, Durinx C, Bal G, Senten K, Augustyns K, et al. Kinetic investigation of chemokine truncation by CD26/dipeptidyl peptidase IV reveals a striking selectivity within the chemokine family. J Biol Chem 2001;276:29839–45.

[23] Tammen H. Specimen collection and handling: standardization of blood sample collection. Methods Mol Biol 2008;428:35–42.

[24] Vidal R, Frangione B, Rostagno A, Mead S, Revesz T, Plant G, et al. A stop-codon mutation in the BRI gene associated with familial British dementia. Nature 1999;399:776–81.

[25] Hopsu-Havu VK, Glenner GG. A new dipeptide naphthylamidase hydrolyzing glycyl-prolyl-beta-naphthylamide. Histochemie 1966;7:197–201.

[26] Hanski C, Huhle T, Reutter W. Involvement of plasma membrane dipeptidyl peptidase IV in fibronectin-mediated adhesion of cells on collagen. Biol Chem Hoppe Seyler 1985;366:1169–76.

[27] Bermpohl F, Loster K, Reutter W, Baum O. Rat dipeptidyl peptidase IV (DPP IV) exhibits endopeptidase activity with specificity for denatured fibrillar collagens. Fed Euro Biochem Soc Lett 1998;428:152–6.

[28] Loster K, Zeilinger K, Schuppan D, Reutter W. The cysteine-rich region of dipeptidyl peptidase IV (CD 26) is the collagen-binding site. Biochem Biophys Res Commun 1995;217:341–8.

[29] Amy Sang Q-X, Shi Y-B. Collagenase 4. In: Barett AJ, Rawlings ND, Woessner JF, editors. Handbook of proteolytic enzymes. 2nd ed., London, San Diego: Elsevier Academic Press; 2004. p. 494–7.

[30] Cawston TE. Collagenase 1. In: Barett AJ, Rawlings ND, Woessner JF, editors. Handbook of proteolytic enzymes. 2nd ed., London, San Diego: Elsevier Academic Press; 2004. p. 472–80.

[31] Henriet P, Eeckhout Y. Collagenase 3. In: Barett AJ, Rawlings ND, Woessner JF, editors. Handbook of proteolytic enzymes. 2nd ed., London, San Diego: Elsevier Academic Press; 2004. p. 486–94.
[32] Tschesche H, Pieper M, Wenzel H. Neutrophil collagenase. In: Barett AJ, Rawlings ND, Woessner JF, editors. Handbook of proteolytic enzymes. 2nd ed., London, San Diego: Elsevier Academic Press; 2004. p. 480–6.
[33] Tiruppathi C, Miyamoto Y, Ganapathy V, Roesel RA, Whitford GM, Leibach FH. Hydrolysis and transport of proline-containing peptides in renal brush-border membrane vesicles from dipeptidyl peptidase IV-positive and dipeptidyl peptidase IV-negative rat strains. J Biol Chem 1990;265:1476–83.
[34] Tiruppathi C, Miyamoto Y, Ganapathy V, Leibach FH. Genetic evidence for role of DPP IV in intestinal hydrolysis and assimilation of prolyl peptides. Am J Physiol 1993;265:G81–9.
[35] Natori Y, Shindo N, Natori Y. Proteinuria induced by anti-dipeptidyl peptidase IV (gp108); role of circulating and glomerular antigen. Clin Exp Immunol 1994;95:327–32.
[36] Thielitz A, Vetter RW, Schultze B, Wrenger S, Simeoni L, Ansorge S, et al. Inhibitors of dipeptidyl peptidase IV-like activity mediate antifibrotic effects in normal and keloid-derived skin fibroblasts. J Invest Dermatol 2008;128:855–66.
[37] Choi SI, Vidal R, Frangione B, Levy E. Axonal transport of British and Danish amyloid peptides via secretory vesicles. Fed Am Soc Exp Biol J 2004;18:373–5.
[38] Lambeir AM, Proost P, Scharpe S, De Meester I. A kinetic study of glucagon-like peptide-1 and glucagon-like peptide-2 truncation by dipeptidyl peptidase IV, in vitro. Biochem Pharmacol 2002;64:1753–6.
[39] Mentlein R, Gallwitz B, Schmidt WE. Dipeptidyl-peptidase IV hydrolyses gastric inhibitory polypeptide, glucagon-like peptide-1(7–36)amide, peptide histidine methionine and is responsible for their degradation in human serum. Eur J Biochem 1993;214:829–35.
[40] Lambeir AM, Durinx C, Proost P, Van Damme J, Scharpe S, De Meester I. Kinetic study of the processing by dipeptidyl-peptidase IV/CD26 of neuropeptides involved in pancreatic insulin secretion. Fed Euro Biochem Soc Lett 2001;507: 327–30.
[41] Kim J, Onstead L, Randle S, Price R, Smithson L, Zwizinski C, et al. Abeta40 inhibits amyloid deposition in vivo. J Neurosci 2007;27:627–33.
[42] Ghiso JA, Holton J, Miravalle L, Calero M, Lashley T, Vidal R, et al. Systemic amyloid deposits in familial British dementia. J Biol Chem 2001;276:43909–14.
[43] Scientific discussion (Sitagliptin). London: European Medicines Agency; 2007. p. 1–39.